

Photonic Crystal Slab Biosensors and its Applications

Utku ERDİVEN*¹, Faruk KARADAĞ¹

¹Çukurova Üniversitesi, Fen Edebiyat Fakültesi, Fizik Bölümü, Adana

Geliş tarihi: 04.01.2017

Kabul tarihi: 14.03.2017

Öz

Bu çalışmada, fotonik kristalden tasarlanan biyosensör cihazı için rezonans frekansını değiştiren sıvı ortamın kırılma indisine ve titanyum dioksit (TiO₂) birim hücre içindeki küresel gümüş metal nanopartikülünün yarıçapına bağlı olarak değişen dolgu faktörü, duyarlılık, kalite faktörü ve lokal yoğunluk incelendi. Bu yapı tipik olarak protein-protein etkileşimi, ilkel hücrelerin görüntülenmesi, kanser hücresi metastazının var olup olmadığının, enzim ve Deoksiribonükleik asit (DNA) mikrodizilerin belirlenmesi için kullanılır. Önerilen hesaplamalar, rezonant dalga boyundaki kaymayı görmek için iki boyutlu TiO₂ fotonik kristal yapısında yaratılan boşluklarının kare örgüsünü ve hava boşluklarına yerleştirilen küçük bir küresel nanopartikülünü kapsamaktadır. Hesaplamalarda örgü sabiti olarak (a= 1 µm) kullanıldı. Analizler 1500-1550 nm dalga boyu aralığında yapıldı. Hesaplamalar, MIT Elektromanyetik Denklem Yayılımına dayalı zamanda sonlu farklar yöntemi yazılımı ile yapılmıştır.

Anahtar Kelimeler: Fotonik kristal, Optik biyosensör, Kalite faktörü, Duyarlılık, Rezonans dalgaboyu

Photonic Crystal Slab Biosensors and its Applications

Abstract

In this study, filling factor, sensitivity, quality factor, and local density of states variation depending on resonance frequency changing refractive index of liquid medium and radius of spherical silver metal nanoparticle inside unit cell for titanium dioxide (TiO₂) photonic crystal slab biosensor device is investigated. This structure is typically used for protein-protein interaction, display of primitive cells, cancer cell metastasis, enzyme detection, Deoxyribonucleic acid (DNA) microarrays. Proposed calculations include a square lattice of air holes created in two-dimensional TiO₂ photonic crystal structure and a small spherical sphere nanoparticle into the air holes is put in order to see shift in resonant wavelength's. Lattice constant (a= 1 µm) was used in the calculations. Analyses have been performed in the wavelength range of 1500-1550 nm. The calculations were made by software MIT Electromagnetic Equation Propagation based finite-difference time-domain method.

Keywords: Photonic crystal, Optical biosensor, Quality factor, Sensitivity, Resonant wavelength

*Sorumlu yazar (Corresponding author): Utku ERDİVEN, ufuk@cu.edu.tr

1. INTRODUCTION

Photonic crystals (PCs) are periodically arranged dielectric structures investigating interaction between biomolecules in two or three dimensions [1]. If periodic parameters (for example, lattice constant, thickness of structure) and refractive index (RI) of photonic crystal (PC) is suitably selected, it will particularly match energy at specific wavelengths. With a capture alternative of insulator fabrics and properties, resonating manners of a PC can be organized to happen at particular arrays of angle and wavelength. This situation admits electromagnetic radiation of chosen wavelength and incident direction to match to the PC and induce an extremely localized electromagnetic stationary wave with amplitude that is considerably bigger than the original clarification source. Heightened irritation will take place by localizing emitters inside the part with a raised electric field magnitude at their innervation wavelength. For the directed modes will match in and out of the PC under phase checking circumstances for particular combining of wavelength and incident angle, it is likely to gather electromagnetic wave at the outcoupling angle further expeditiously, and hence supplying a heightened eradication physical, chemical and biologic device [2]. To summarize, while the PC is enlightened with a wideband wave source, catching diffraction modes match electromagnetic radiation into and out of structure having high dielectric constant, disruptively interfering with the carried light. At a peculiar resonant wavelength and incident angle, absolute intervention happens and any light is not conveyed (100% reflection is almost occur). The resonant wavelength is regulated by the increase of biomaterial upon the PC optical biosensor surface, resulting in a displacement to a greater wavelength. The electromagnetic wave that is produced at the PC surface during resonant light matching prohibits sidelong spread [3].

Accordingly, there are many applications such as display of primitive cells [2], cancer cell metastasis, biofilm and gene identification [4], biomolecular detection [5], DNA microarrays, and pharmaceutical drug screening [6-8]. These

structures including cavities can be also used as label-free PC biosensors (kinetic imaging of cell-surface interactions) [9], immobilized protein targets [10].

Label-free biodetectors achieve on accommodate by a couple of important physical ability link to observing biomolecular fundamental interactions and organic analytes that can admit appropriate particles, peptides, proteins, bacterium, or stem cells [11]. Label-free sensing elements are supported a regular design or construction of insulator substance in two or three dimensions optimized to supply a highly constricted resonating mode whose wavelength is especially sensible to inflections caused by the deposit of biochemical material on its plane [12]. In fact, the detector surface is lighted with white light and the mirrored light from dissimilar positions is assembled. When the variations in the wavelength of the reflected electromagnetic radiation are analyzed, biochemical binding cases happening on the sensing element surface can be noticed and measured. Generally, label-free biosensing with optics depends on observing exchanges in a particular parametric quantity such as absorption, reflection, index of refraction.

TiO₂ has been generally applied for another practice such as electrochemical impedance spectroscopy [13], single nanoparticle detection [14], visible wavelength emitting quantum dots [2], screening of immobilized protein enzymes [3] and atomic layer deposition [10] and electrochemical biodetector applications [11]. However, TiO₂ has wide photonic band range and optic assimilation stage is ten times less than that of the silicon at optic communicating wavelength (1.5 μm), it can restrain more easily to the led resonance modes. It has especially a high sensitivity at the near-infrared (750 nm) and near-ultraviolet (400 nm) wavelengths [2]. Therefore, TiO₂ can be used to immobilizing proteins, enzymes in biomolecular material and optical biosensor practices [14]. Beside this, TiO₂ shows the increase of a liquid based fluorescence assay component from photonic crystal optical biosensor [15]. Fluorescence is an important application area for assay of biological structures such as DNA

identification and protein diagnostic analysis. At the same time, with TiO₂ layer which has 60 nm thicknesses can be observed both attachment footprints of filopodial extensions and intracellular attachment strength gradients [3]. TiO₂ PC slab structure is quite a significant mechanism of nanoscale PC optical biosensors. Because, in such a case, the high RI dielectric slab limits guided modes of electromagnetic wave and it couples the allowed incident optical beams at the guided resonance frequencies [16, 17].

In this study, we explain the theoretical features of RI detection in PCs optical biosensor materials to improvement of present analyzes of TiO₂ photonic crystal-based sensor devices. We calculate features for directed resonance modes connected on these devices and specify that the type of headed resonance mode promoted by the PC slab can solution in notably other detection properties. This distinction is particularly important in symmetric or asymmetric PCs optical biosensor structures, in which the slab is suspended in water or other liquids. While coated with the same liquid (water, alcohol vs.) both sides (bottom and top) of the symmetric PC (SPC) slab (TiO₂) structure having a high RI, in the asymmetric PC (APC) structure bottom side of the slab is supported by SiO₂.

Our studies are promoted as follows. Part 2 gives short information about calculation techniques containing our workings. Part 3 explains sensitivity, filling fraction, quality factor, local density of states (LDOS) and frequency values of the guided resonance modes about symmetric and asymmetric TiO₂ PC biostructures. TE-like guided resonance modes in PCs optical biosensors are described in Part 3. In this section, we will obtain transmission spectra of TE-like directed resonance modes within symmetric and asymmetric structures and we will compare our found results in the end.

2. MATERIALS AND METHODS

To understand the operation of PC biosensors, some important biometric parameters must be explained. These parameters are sensor sensitivity, detection limit or resolution, quality factor, filling

fraction. Sensor sensitivity is specified as the ratio of the alteration in sensing element output response to the exchange in the measure to be evaluated.

Sensitivity of the sensor is influenced from a few factors such as thickness of the slab and RI. This sensitivity is basically specified with the interaction between biomolecules and electromagnetic field for PC optical biosensors. It has been also explained by density of electromagnetic radiation at the biosensor surface. In this situation, fraction of the light in the solution affects sensor's sensitivity.

For all that, guided resonance modes in the sensing mechanism can be replaced in the spectral position. For this, the amount of liquid and analytes binding to the biological material or the refraction of index of the medium surrounding the PC slab must be changed with external influences. So, PC optical biosensor structure can be stimulated at the guided resonance frequencies. Because, the real interaction between the generated layer with electromagnetic field energy occurs in these frequencies. These cases cause shift of the PC sensing element structure directed resonances. As a result, bulk spectral sensitivity can be calculated as follows [18].

$$S = \frac{\Delta\lambda}{\Delta n_{liquid}} = f \frac{\lambda_0}{n_{eff}} \left[\frac{nm}{RIU} \right] \quad (1)$$

Here, while $\Delta\lambda$ is spectral shift of guided resonance modes λ_0 , Δn , n_{eff} , f defines resonance wavelength, RI change of liquid, effective index of refraction of the dielectric detecting device and filling fraction of light, respectively. In addition, LDOS of the resonance modes can be calculated since spherical silver is placed inside the proposed structure. Therefore, the LDOS could be made definitions on the fluorescence properties of biosensor device looking at the Purcell enhancement effect. In this case, the LDOS of guided resonance's [19] can be defined as,

$$LDOS \approx \frac{2}{\pi\omega^n} \frac{Q^n}{V^n} \quad (2)$$

Where, Q is the dimensionless quality factor and V is the modal volume of modes.

As shown in Figure 1, PC structure depicts periodically arranged dielectric slab device. This device may be completely specified by a unit cell with a lattice constant, r' hole radius, r spherical silver radius and t thickness, n refractive index. In the forming structure, titanium dioxide (TiO_2 , $n= 2.62$) has high RI surrounds with a low RI fluid namely water ($n= 1.33$), isopropyl alcohol (IA) ($n= 1.3776$), ethanol ($n= 1.3611$) and hydrogen peroxide (HP) ($n= 1.4061$). Polarization parameters of the spherical silver are founded in MIT Electromagnetic Equation Propagation MEEP units [20].

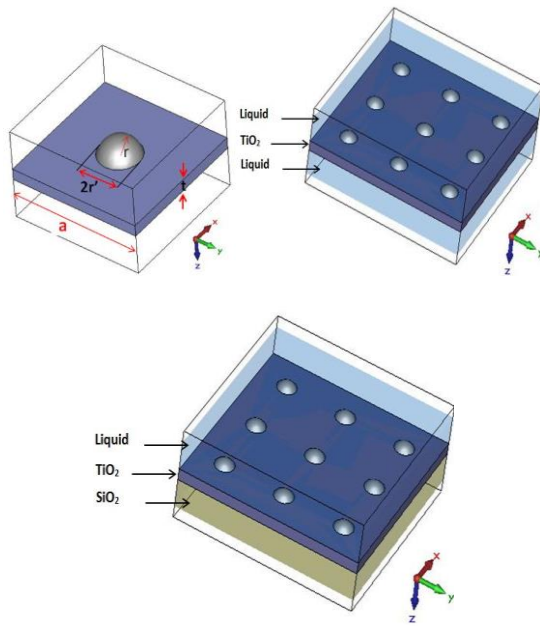


Figure 1. Illustrations of a unit cell, SPC and APC design for a square grid of holes PCS, respectively. In SPC device, while TiO_2 slab has high RI, the index of refraction of the medium surrounding the TiO_2 slab is lower than TiO_2 . In the TiO_2 , APC slab is promoted SiO_2 substrate which has a RI higher than liquids, lower than TiO_2 . The diameter of the holes ($2r'$) is $0.3a$. The radius of the spherical silver (r) is $0.1a$. The thickness of TiO_2 slab (t) is $0.2a$.

Computational technique is used by MEEP [21] using “dimensionless” units, a freely available finite difference time-domain (FDTD) implementation. The FDTD is an accurate method for determining the interaction of any physical structure with electromagnetic radiation. The electric field of the transverse electric (TE) polarization is parallel to the 2D plane of the structure, normal to the magnetic field vector H_z following the normal PC device [22]. Periodic boundary conditions with FDTD can be applied a single unit cell. These boundary conditions are implemented to xz and yz planes to obtain infinite planar periodicity while perfect matched layers (PMLs) restrict the top and bottom of the unit cell to engulf outgoing fields. To analyze modes of the PC slab in the periodic boundary condition, the irradiation occurs of a wideband planar Gaussian source was placed above the periodic boundary condition. Modal field dispersions are calculated by stimulating the PC slab utilizing a planar continuous light source also positioned above the PC slab.

3. RESULTS AND DISCUSSIONS

Symmetrical and asymmetrical structure of TiO_2 PC biosensor application in the square lattice of holes is provided in Figure 1. In SPC device, the index of refraction of the medium surrounding the TiO_2 slab is lower than TiO_2 while TiO_2 slab has high RI. In TiO_2 APC slab is promoted SiO_2 substrate which has a RI higher than liquids and lower than TiO_2 . The spherical silver material was placed within the center of holes for both symmetrical and asymmetrical structures.

Transmission spectra of the symmetric biosensor structure of different surrounded mediums excited at the guided resonance frequencies, (the thickness of slab, the radius of holes and the radius of silver sphere is $0.2a$, $0.3a$, $0.1a$, respectively) are shown in Figure 2. According to the working principle of the PC biosensor's, the change in RI of the liquids causes very small spectral shifts of the resonance frequencies. While the increasing of the RI of the fluid in the vicinity of the slab causes decreasing the frequency of the TE-like guided modes, it ensures increasing of the quality factor. So, both

scattering in PC slab decreases and more interaction between proposed structures with electromagnetic radiation occurs. In this situation, filling factor and sensitivity values increase. As given in Table 1, especially, fluorescence properties of PC biosensor enhance under influence of the effective RI. As a result, PC slab sensors incorporate these precious features with the skill to couple light from free-space radiation modes into directed resonances by perpendicular light coupling.

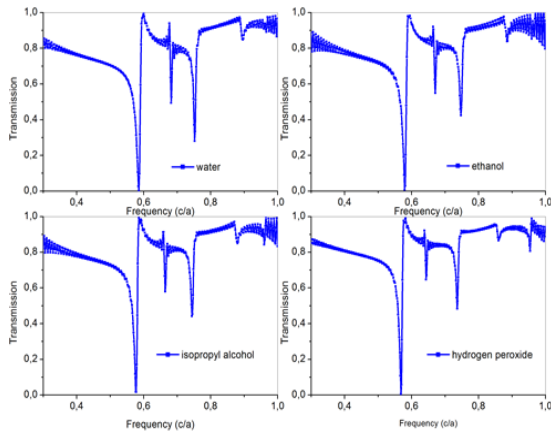


Figure 2. TE-like mode transmission spectrum for silver sphere radius $r = 0.1a$ and hole radius $r = 0.3a$ for SPC

Table 1. Results of the symmetric photonic crystals. The radius of the holes is $0.3a$. The radius of the spherical silver is $0.1a$. The thickness of slab is $0.2a$. (IA- Isopropyl Alcohol, HP- Hydrogen Peroxide)

Materials (liquid)	Resonance wavelength (nm)	Sensitivity (nm/RIU)	Quality factor	Filling fraction	LDOS
Water	1710	162	54	0.248	37
Ethanol	1724	450	60	0.683	42
IA	1733	545	188	0.823	134
HP	1751	630	374	0.942	270

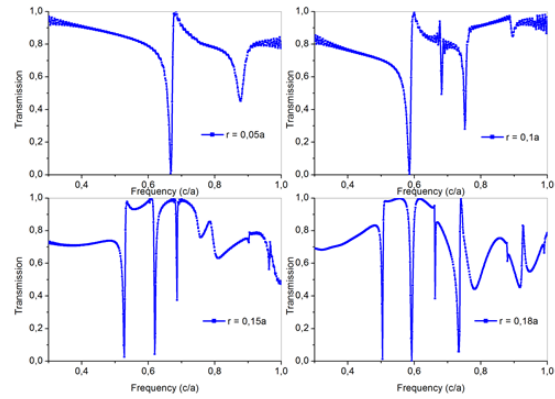


Figure 3. SPC TE-like mode transmission spectrum for water medium. The changed radius of spherical silver metal creates small shifts at the guided resonance frequencies

Table 2. Results of the symmetric photonic crystals. Water was used as a liquid. The radius of the holes is $0.3a$

Radius (r)	Thickness of slab	Resonance wavelength(mm)	Sensitivity (nm/RIU)	Quality factor	Filling fraction	LDOS
0.05a	0.1a	1500	108	1298	0.188	806
0.1a	0.2a	1710	162	54	0.248	40
0.15a	0.3a	1893	141	1020	0.195	782
0.18a	0.36a	1984	70	143	0.092	115

Transmission spectra of symmetric biosensor structure of surrounded same liquid medium (water) excited at the guided resonance frequencies are shown in Figure 3. The increasing simultaneously of the radius of silver spheres and the thickness of the slab has been effected in a different manner to the variation of the effective index of refraction as seen in Table II. While the radius of the silver metal spheres is $0.15a$ and $0.18a$ the number of the obtained resonance frequencies is more than others as seen in Figure 3. This case effectively enriches the fluorescence and sensing properties of the biodetecting structure.

Same conditions happen in APC slab device. When APC and SPC biosensor structure is

compared, the guided resonance frequencies of APC sensing element are shifted to smaller values. Transmission spectra for APC slab designs and surrounded liquid medium excited at TE-like directed resonance mode frequencies are provided in Figure 4. These obtained values are also summarized in the Table 3.

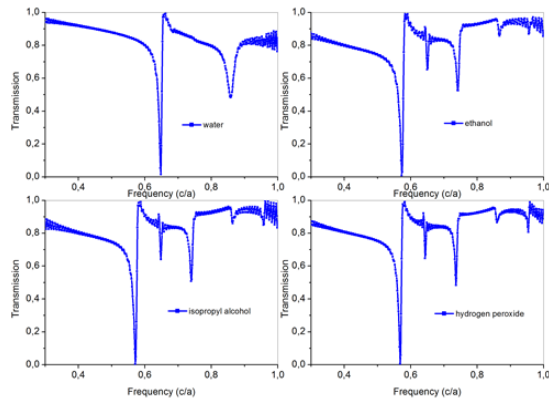


Figure 4. TE-like mode transmission spectrum in APC slab for silver sphere radius $r = 0.1a$ and hole radius $r = 0.3a$

Table 3. Results of the asymmetric photonic crystals. The radius of the holes is $0.3a$. The radius of the spherical silver is $0.1a$. The thickness of slab is $0.2a$. (IA- Isopropyl alcohol, HP- Hydrogen Peroxide)

Materials (liquid)	Resonance wavelength (nm)	Sensitivity (nm/RIU)	Quality factor	Filling fraction	LDOS
Water	1736	180	57	0.271	40
ethanol	1748	300	62	0.450	43
IA	1751	315	65	0.470	45
HP	1760	385	70	0.573	50

With the increase of the RI of the liquid in the small volume the relative RI decreases. Hence, the interaction between the implemented electric field energies and liquids rises. Result of that the values of sensitivity, quality factor, filling fraction and LDOS increase, as provided in Table 3.

In APC slab, the transmission spectra caused by the increase of the silver sphere and the thickness of the slab are given in Figure 5. According to Table 4, the calculated LDOS exhibits the better results compared with Figure 3. This situation shows the improved fluorescence features of the biodetecting structure.

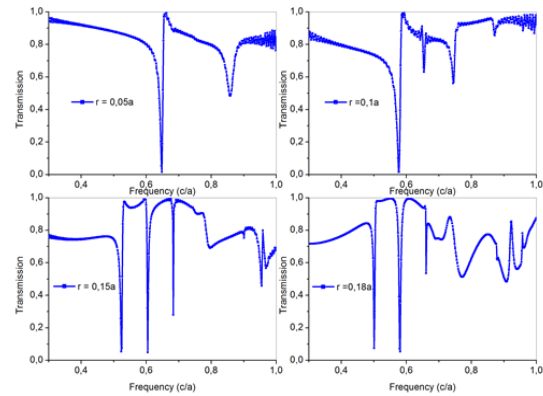


Figure 5. TE-like mode transmission spectrum in APC slab for water medium. The changed radius of spherical silver metal creates small shifts at the guided resonance frequencies

Table 4. Results of the asymmetric photonic crystals. Water was used as a liquid

Radius (r)	Thickness of slab	Resonance wavelength (nm)	Sensitivity (nm/RIU)	Quality factor	Filling fraction	LDOS
0.05a	0.1a	1543	124	140	0.210	85
0.1a	0.2a	1736	180	57	0.271	40
0.15a	0.3a	1912	136	106	0.186	78
0.18a	0.36a	2000	266	142	0.089	115

Thus, the obtained results show that they appropriately provide interaction between electromagnetic waves and biosensing element region. TE-like guided resonances penetrate effectively to external regions of TiO_2 slab. So, the proposed structures can be optimized for protein-protein interaction, enzyme detection, molecular diagnostics, small molecule aggregation and inhibition of protein-DNA interactions.

4. CONCLUSION

In conclusion, effect of the RI of the liquid medium and the small spherical silver placed inside TiO₂ slab are investigated. It demonstrates that the changing radius of the silver sphere increase the number of reflected resonant wavelength in the PC's and at the same time, this situation shows that silver spheres not only shift the guided resonance frequency, but also optical absorption of PC's essentially decrease. The obtained graphs for index of refraction change of 0.01 will create a change of approximately 0.001 in the guided resonant frequencies. Thus, the proposed TiO₂ biosensor structure has high sensitivity, quality factor and LDOS at the visible wavelengths.

5. REFERENCES

1. Yun, M., Wan, Y., Liang, J., Xia, F., Liu, M., Ren, L., 2012. Multi-Channel Biosensor Based on Photonic Crystal Waveguide and Microcavities, *Optik*, vol. 123, pp. 1920-1922.
2. See, G. G., Naughty, M. S., Tang, T., Bonita, Y., Joo, J., Trefonas, P., Deshpande, K., Kenis, P. J. A., Nuzzo, R. G., Cunningham, B. T., 2015. Region Specific Enhancement of Quantum Dot Emission using Interleaved Two-Dimensional Photonic Crystals, *Applied Optics*, vol. 54, no. 9, pp. 2302-2308.
3. Chen, W., Long, K. D., Lu, M., Chaudhery, V., Yu, H., Choi, J. S., Polans, J., Zhuo, Y., Harley, B. A., Cunningham, B. T., 2013. Photonic Crystal Enhanced Microscopy for Imaging of live cell adhesion, *Analyst*, vol. 138, no. 20, pp. 5886-5894.
4. Cunningham, B. T., Zhang, M., Zhuo, Y., Kwon, L., Race, C., 2014. Review of recent advances in Biosensing with Photonic Crystals, *IEEE Sensors Journal*, 2014 IEEE Sensors Conference, Doi. 10.1109/JSEN.2015.2429738, April 2015.
5. Zhang, M., Peh, J., Hergenrother, P. J., Cunningham, B. T., 2014. Detection of Protein-Small Molecule Binding using a Self-Referencing External Cavity Laser Biosensor, *J. Am. Chem. Soc.*, vol. 136, pp. 5840-5843.
6. Peterson, R. D., Cunningham, B. T., Andrade, J., 2014. A Photonic Crystal Biosensor Assay for Ferritin Utilizing Iron-Oxide Nano Particles, *Biosens. and Bioelectron.*, Vol. 56, pp. 320-327.
7. Shamah, S. M., Cunningham, B. T., 2011. Label-free Cell-based Assays using Photonic Crystal Optical Biosensors, *Analyst*, vol. 136, pp. 1090-1102.
8. Tan, Y., Sutanto, E., Alleyne, A. G., Cunningham, B. T., 2014. Photonic Crystal Enhancement of a Homogeneous Fluorescent Assay using Submicron Fluid Channels Fabricated by E-jet Patterning, *J. Biophotonics*, Vol. 3-4, pp. 266-275.
9. Pineda, M. F., Chan, L. L., Kuhlenschmidt, T., Kuhlenschmidt, M., Cunningham, B. T., 2009. Rapid Label-free Selective Detection of Porcine Rotavirus using Photonic Crystal Biosensors, *IEEE Sensors Journal*, vol. 9, no. 4, pp. 470-477.
10. Jardinier, E., Pandraud, G., Pham, M. H., French, P. J., Sarro, P. M., 2009. Atomic Layer Deposition of TiO₂ Photonic Crystal Waveguide Biosensors, *J. Phys., Conf. Series* 187, 012043.
11. Kafi, A. K. M., Wu, G., Chen, A., 2008. A Novel Hydrogen Peroxide Biosensor Based on the Immobilization of Horseradish Peroxidase onto Au-modified Titanium Dioxide Nanotub Arrays, *Biosens. Bioelectron.*, vol. 24, pp. 566-571.
12. Cunningham, B. T., Li, P., Schulz, S., Lin, B., Baird, C., Gerstenmaier, J., Genick, C., Wang, F., Fine, E., Laing, L., 2004. Label-free Assays on the BIND System, *J. Biomol. Screen.*, vol. 9, pp. 481-490.
13. Na, Z., Tao, Y., Kui, J., Cai-Xia, S., 2010. Electrochemical Deoxyribonucleic Acid Biosensor Based on Multiwalled Carbon Nanotubes/Ag-TiO₂ Composite Film for Label-Free Phosphinothricin Acetyltransferase Gene Detection by Electrochemical Impedance Spectroscopy, *Chin. J. Anal. Chem.*, vol. 38, no. 3, pp. 301-306.
14. Zhuo, Y., Hu, H., Chen, W., Lu, M., Tian, L., Yu, H., Long, K. D., Chow, E., W. King, P., Singamaneni, S., Cunningham, B. T., 2014. Single Nano Particle Detection using Photonic

- Crystal Enhanced Microscopy, *Analyst*, vol. 139, no. 5, pp. 1007-1015.
15. Chaudhery, V., George, S., Lu, M., Pokhriyal, A., Cunningham, B.T., 2013. Nanostructured Surfaces and Detection Instrumentation for Photonic Crystal Enhanced Fluorescence, *Sensors*, vol. 13, pp. 5561-5584.
 16. Johnson, S. G., Fan, S. H., Villeneuve, P. R., Joannopoulos, J. D., Kolodziejski, L. A., 1999. Guided Modes in Photonic Crystal Slabs, *Phys. Rev. B.*, vol. 60. no. 8, 5751–5758.
 17. Fan, S., Joannopoulos, J. D., 2002. Analysis of Guided Resonances in Photonic Crystal Slabs, *Phys. Rev. B.*, vol. 65 no. 23, pp. 235112(1)-235112(8).
 18. Mortensen, N. A., Xiao, S. S., Pedersen, J., 2008. Liquid-infiltrated Photonic Crystals: Enhanced Light-Matter Interactions for Lab-on-a-chip Applications, *Microfluid. Nanofluid.*, vol. 4, no. 1-2, pp. 117–127.
 19. Qiu, P., Wang, G., Lu, J., Wang, H., 2012. Local Density of States in Photonic Crystal Cavity, *Front. Optoelectron.*, vol. 5, no. 3, pp. 341-344.
 20. <http://ab-initio.mit.edu/MEEP/Tutorial>,
 21. Oskooi, A. F., Roundy, D., Ibanescu, M., Bermel, P., Joannopoulos, J. D., Johnson, S. G., 2010. MEEP: A Flexible, Free-software Package for Electromagnetic Simulations by the FDTD Method, *Comput. Phys. Commun.*, vol. 181, pp. 687–702.
 22. Joannopoulos, J. D., Meade, R. D., Winn, J. N., 1995. *Photonic Crystals: Molding the Flow of Light*, University Press, Princeton.